LA-UR -82-1397

Conf-820644--2

Los Alamos National Laboratory is operated by the University of California for the United States Department of Energy under contract W-7405-ENG-36.

TITLE: COMPACT TOROID EXPERIMENTS: SPHEROMAKS AND FIELD-REVERSED CONFIRGURATIONS

AUTHOR(S) W. E. Quinn, CTR-DO

LA-UR--82-1397

DE82 015802

SUBMITTED TO Journal of Nuclear Instruments & Methods
Contributed paper for "Symposium on New Trends in Unconventional Approaches to Magnetic Fusion" to be held June 16-18, 1982, Stockholm, Sweden.

Los Alamos Los Alamos National Laboratory
Los Alamos, New Mexico 87545

COMPACT TOROID EXPERIMENTS: SPHEROMAKS AND FIELD REVERSED CONFIGURATIONS

WARREN E. QUINN AND COMPACT TOROID STAFF

Los Alamos National Laboratory, Los Alamos, New Mexico, 87545, U.S.A.*

Compact toroids (CT) containing both poloidal and toroidal magnetic field, spheromaks, are generated in the CTX experiment using a magnetized coaxial plasma gun, and are trapped and stably confined in an oblate flux conserver. Total configuration lifetimes are observed up to ~ 0.8 ms, consistent with classical resistive decay. The field reversed configuration (FRC) is a high beta, axisymmetric, highly prolate compact toroid, containing only poloidal magnetic field, formed in a field-reversed theta pinch. A quiescent confinement period of 30 to 90 μs with T_i ~ 200-500 eV and n ~ 5×10^{15} cm^{-3} is terminated by an n=2 rotational instability. The FRC is stable to MHD modes including the tilting instability.

I. INTRODUCTION

A compact toroid (CT) is an axisymmetric, closed toroidal magnetic-confinement configuration that has no magnet coils, conducting walls, nor vacuum walls linking the hole in the plasma torus.[1] This feature provides a simple geometry that reduces engineering complexity in proposed CT reactors. The CTs can be classified into three major types; particle rings (Astron-like), spheromaks, and field reversed configurations (FRC). Particle rings are characterized by large ratios of ion gyroradius to plasma dimensions, and may have arbitrary ratios of toroidal to poloidal magnetic fields. Both the spheromak and the FRC have small gyroradii compared with plasma dimensions. The spheromak has poloidal and toroidal magnetic field components of comparable magnitude on the closed flux surfaces. The flux surfaces of the FRC have purely poloidal field lines. Open field lines exist between the separatrix and an external cylindrical conductor. The CT equilibrium requires either a conducting wall or an externally generated field, like the vertical field in a tokamak. If an external field is used, a separatrix is formed that divides these open field lines from the closed fields supported by plasma currents in the toroid. The toroidal confinement properties of CT configurations are complementary to other axisymmetric devices. In contrast to the modest shear and minimum B of the tokamak, the spheromak, like the reversed field pinch (RFP), has stronger shear and no minimum B. We report on spheromaks and FRCs studied at the Los Alamos National Laboratory in the CTX spheromak facility, and in two field reversed theta-pinch experiments FRX-B and FRX-C.

II. COMPACT TOROIDS WITH TOROIDAL FIELD: SPHEROMAKS

A. Formation

Spheromaks have been generated in the Los Alamos CTX facility using a magnetized coaxial plasma gun.[2] The gun is 1.2 m in length with inner and outer electrode radii of 0.10 m and 0.15 m, respectively; and is energized by a 45-kV, 37-μF capacitor bank. The CTs are generated utilizing in part a technique pioneered by Alfvén et al.[3] and extended to a higher-temperature fully ionized plasma regime. A solenoidal coil produces an axial magnetic field inside the inner electrode that diverges at the gun muzzle and becomes radial. Firing the gun

*Work performed under auspices of U.S. Department of Energy.

produces a radial plasma current that generates a toroidal magnetic field between the electrodes. The $\vec{J}\times\vec{B}$ force accelerates the highly conductive plasma out of the gun, stretching the radial field lines in the axial direction away from the gun. These elongated field lines reconnect behind the plasma forming the closed poloidal field of the CT spheromak, while the magnetic field generated by the gun current and embedded in the plasma becomes the toroidal field. The gun-generated spheromaks are trapped in prolate and oblate cylindrically symmetric metallic flux conservers.

B. Gross Stability and Plasma Characteristics

In the initial experiments,[2] the gun-generated spheromaks were injected into a stainless steel, right-circular, cylindrical flux observer. The CTs were stopped within the flux conserver by appropriate adjustment of the initial poloidal field strength at the coaxial source. In some cases the toroid stopped with its major axis parallel to the axis of the plasma gun and the flux conserver, then rotated 90° so that its axis was orthogonal to the axis of symmetry. This tilting mode had been predicted by Rosenbluth and Bussac.[4] In most cases the stopped toroid, when first observed, was already partially tilted. After the rotation or tilting, the deformed toroid appeared grossly MHD stable with a lifetime of ~ 100 μs.

Motivated by stability theory,[4] which predicts that the tilting mode should be stabilized by an oblate flux conserver, compact toroids were trapped in 80-cm diameter flux conservers having oblate regions.[1] The tilting instability does not occur and the spheromak configuration is stable throughout its lifetime, although the instability is sensitive to the geometry of the entrance cylinder to the flux conserver and the gap spacing between the gun and the entrance region.[1] The plasma and magnetic field properties are measured using magnetic probes, Thomson scattering, interferometry, bolometry, and quartz UV spectroscopy. The electron density and temperature of the separated, trapped spheromak are typically $n_e \sim 2\text{-}4\times10^{14}$ cm^{-3} and $T_e \sim 10$ eV. Probes measuring all three components of magnetic field located along the axis of symmetry show that magnetic reconnection, leading to separation of the spheromak from the coaxial source, is completed by 40 μs. The peak field on the axis of symmetry is ~ 6 kG, and the total energy of the spheromak is ~ 6 kJ. Total lifetimes of the spheromak configuration are observed up to 0.8 ms (~ 4 times the characteristic decay time) and are consistent with classical resistive decay.

C. Relaxation toward a Taylor Minimum Energy State

Radial profiles of the poloidal and toroidal magnetic fields are found to be in approximate agreement with those of the Taylor minimum energy state theory,[5] although some deviations are observed. These Taylor-like states, similar to those in the Reversed Field Pinch[6] (RFP), have been calculated and are consistent with the observed conversion of toroidal flux into poloidal flux without a global disruption. RFP experiments show that stable high β (10-20%) states lie near the predictions of Taylor's $\beta = 0$ model for $B_{Toroidal}(wall) < 0$, and the configuration regenerates itself against diffusive losses.[6] The RFP plasmas move into the reversed-field area, dwell there, move out by field diffusion, and then relax back to the reversed-field region.

In the CTX spheromak, a similar relaxation phenomenon is observed. In Fig. 1, the measured ratio of the toroidal field just outside the magnetic axis to the poloidal field on the major axis are plotted as a function of time. This ratio is compared with the calculated ratio for the Taylor state (dashed line). There is agree-

ment following the spheromak formation, but in time the measured ratio deviates by as much as 50 percent and then a relaxation process restores the plasma configuration back to the Taylor minimum energy state as shown in Fig. 1. Thus, the equilibrium configuration tends to regenerate itself against diffusive losses. A 2-D transport code developed by Sgro[7] shows magnetic diffusion resulting in the observed rate of deviation of the ratio from the Taylor value as indicated by the triangles in Fig. 1, but of course, does not show the 3-D relaxation process.

D. Impurity Radiations

Bolometry and UV spectroscopic measurements have shown that impurity radiation is the dominant energy loss mechanism in the CTX spheromaks. It appears that radiative losses are clamping the temperature in the 10 to 20 eV range. Metallic impurities have been reduced to negligible levels compared with lower Z impurities by appropriate choice of source operating conditions. Earlier spectroscopic line observations[8] indicated large amounts of power were being radiated by carbon and oxygen impurities. A computer code developed by Barnes,[9] to calculate nonequilibrium charge state distributions and radiated power for different impurities, shows that oxygen impurity levels of 5 to 15% are sufficient to radiate the ohmic heating power and clamp the temperature.

The carbon impurity has been reduced to negligible levels, by discharge cleaning and improved vacuum conditions, and the duration of the OIV and OV radiations is significantly increased indicating that the plasma is sufficiently hot to ionize oxygen into these higher states for longer times. These impurity reduction efforts increased the spheromak configuration lifetime from 250 μs to 550 μs. There are several kilojoules of magnetic field energy whose decay could provide, through ohmic heating, temperatures of a few hundred eV in the absence of loss processes. At a reduced oxygen impurity level of 1 to 5%, the radiated power will become less than the available ohmic heating power and the plasma should begin to heat. This should result in a "burn-through" of the oxygen impurity and considerably hotter spheromaks with lifetimes in the millisecond range.

A new operating mode with a constant background fill of several millitorr of H_2 has increased the spheromak configuration lifetime to 0.8 ms. This background gas fill has the following advantageous features:[9] (1) Reduces impurity generation in the gun; (2) Allows stable, well confined spheromaks to be generated at higher poloidal fields and at lower main bank energies, further reducing the impurities; (3) Allows clean operation at short gas puff delays, resulting in lower initial densities and less radiated power; and (4) Provides a particle source to maintain the density at low levels throughout the longer discharge lifetime.

E. Equilibrium and Stability

The equilibrium and the gross MHD stability of the spheromak in an oblate-shaped conducting shell has been extensively studied theoretically[4,10,11] and confirmed experimentally.[1,12] Theory predicts that $r_s/r_c > 0.7$-0.8 is sufficient to stabilize the tilting/sliding modes, and $r_s/r_c > 0.8$-0.9 is sufficient to stabilize all other global MHD modes, where r_s and r_c are the separatrix and conducting wall radii measured from the magnetic axis. The addition of high energy ions to small-orbit CTs has been proposed[13] and theoretically shown to enhance the stability to tilting and other gross modes, thereby reducing the required values of r_s/r_c. These stability limits of wall separation have not yet been systematically studied experimentally, but

stable spheromak configurations are routinely produced in CTX.

The theoretical ideal MHD limit of the engineering beta is relatively high, $\beta_e \sim 0.15$.[14] The Maryland PS-1 device[15] has produced $\beta_e \sim 0.3$, while $\beta_e \sim 0.16$ has been observed in the CTX spheromak experiment.[16] However, the experimental value of β_e that can be achieved with acceptable transport in the collisionless regime has not been determined.

The present substantial understanding of the equilibrium and gross stability of spheromaks indicate nothing to prevent their use in reactors. The oblate wall requirement imposes limits on their usage in moving ring systems, and on the reduction of r_s/r_c in an adiabatically heated system. The injection of high energy ions reduces these limits. The CT is a flexible configuration that allows a variety of applications.

F. Transport, Heating, and Sustainment

The immediate need in present spheromak experiments is to increase the electron temperature so that transport and heating studies can be performed in a relatively collisionless regime ($T_e > 100$ eV). The RFP experimental results indicate that the impurities must be low to allow an operating "window" in density between radiation at high density and drift-induced turbulence at low density. Improved impurity control is being developed in the CTX spheromak experiment so that ohmic heating can increase the temperatures above 100 eV. Higher temperatures will allow collisionless confinement experiments and a variety of heating and sustainment experiments using rf, beams, and adiabatic compression.

III. Field Reversed Configuration (FRC)

An FRC is a prolate toroidal plasma configuration contained by poloidal magnetic field, generated by plasma currents carried by particles with small gyroradius, and with negligible toroidal field. FRCs have been produced in the laboratory since the early 1960s using the field reversed theta pinch, and are represented schematically in Fig. 1 provided the toroidal field is deleted. The FRC is produced by embedding an initial bias field into a cold preionized plasma followed by rapidly reversing the direction of current in the theta-pinch coil. The resulting oppositely directed fields tear and reconnect at the ends, generating the closed field line structure of the FRC. Additional positive flux, generated by the rising magnetic field, produces open field lines separated from the reconnected field lines by a separatrix. A passive crowbar clamps the externally applied field with an e-folding decay time of 100 to 300 μs.

A review of FRC experiments and theory is given in Ref. 17. Work at Los Alamos[18] and at the Kurchatov Institute[19] during the 1970s has been particularly significant. The Kurtmullaev group has studied enhanced field reversal techniques, controlled field reconnection, and axial shock heating. Plasma lifetimes of ~ 100 μs are limited by the decay of the external field, and the energy containment is projected to be ~ 300 μs. The Los Alamos FRX experiments have produced plasma temperatures in the 0.1 to 1 keV range, peak densities of $\sim 5\times10^{15}$ cm^{-3}, and configuration lifetimes of up to 120 μs.

In the last few years a good theoretical understanding has been achieved of the high-beta elongated FRC equilibrium. A useful result, independent of pressure profile, known as the "average beta condition" is the following:[20,21]

$$\langle\beta\rangle = 1 - r_s^2/2r_c^2 \quad (1)$$

where $\langle\beta\rangle$ is the volume average inside the separatrix of $8\pi P/B^2_{ext}$. Stability

is still an important issue for the FRC. Many MHD modes of instability originally expected for the FRC have been found to be stabilized either by the elongated geometry or by finite-Larmar-radius effects often accentuated by the internal field null. An internal m=1 mode similar to spheromak tilting has been predicted theoretically,[22-25] but it has not been observed experimentally. The only instability that occurs experimentally is a destructive n=2 mode that apparently results from a gradual build up of plasma rotation.[25]

A. FRC Experimental Facilities and Results

Table I lists the parameters of Los Alamos FRC experiments.

TABLE I
PARAMETERS OF FRC EXPERIMENTS

Experiment	id/L (cm)	Max. Energy (kJ)	Voltage (kV)	$\tau/_4$ (μs)	B_{MAX} (kG)
FRX-B	20/100	106	55	2.4	11.0
FRX-C	40/200	600	110	5.0	10.0

Both the FRX-B[17] and -C[26] devices have symmetric passive magnetic mirrors (mirror ratios of 1.05 to 1.10) produced by decreasing the inside diameter of the coils near the ends.

Kurtmullaev's group at the Kurchatov Institute produce FRCs in reversed-field theta-pinches using additional magnetic fields to control the formation process.[19] A pulsed octupole barrier field is used to maximize the trapped flux and minimize plasma losses to the wall during the field reversal process. Both mirror and cusp fields are used at the ends of the main coil to control the field reconnection process and to initiate an axial shock compression. The Soviets produce stable FRCs that last the full 100-μs L/R decay time of their magnetic fields and do not observe a rotational instability. The TRX-1 experiment[27] uses many features of the Kurtmullaev experiments including pulsed barrier magnetic fields to maximize flux trapping efficiency, and both cusps and mirror fields to control the reconnection through shaping and rapidly changing the magnetic field configuration at the coil ends.

Experimental efforts have been successful in clarifying many features of the FRC and give the following significant results: (1) An FRC can be created using field reversed theta-pinch techniques. The resistive tearing mode can be controlled by proper vacuum procedures, preionization methods, and experimental design; (2) A weakly compressed FRC inside a conducting wall is observed to be MHD stable; (3) The FRC displays a quiescent phase that is terminated by a growing n=2 mode most likely caused by rotation resulting from non-classical transport; (4) The confinement of plasma and energy during the quiescent period is much superior to plasma confinement in open field line configurations; and (5) Translation of the CT from one coil region to another has been successfully demonstrated.

B. Equilibrium

After the FRC formation, a quiescent stable period of plasma confinement is observed before the onset of the rotational instability. During this stable period the equilibrium profile and parameters have been studied in the FRX-B experiment[17] with a fill pressure of 17 mtorr. The FRC major radius R, determined from end-on framing photographs, is approximately 3.4 cm at t = 9.5 μs, which, assuming pressure balance gives a separatrix radius, $r_s = \sqrt{2}\,R \sim 5.0$ cm. Radial density profiles from Thomson scattering measurements on the axial midplane yield a major radius of R ~ 3.8 cm in reasonable agreement with the end-on luminosity measurements. Excluded flux measurements as

a function of axial position and time give a separatrix radius $r_s \sim 5$ cm assuming the diamagnetic contribution from the plasma on the open field lines is negligible. The excluded flux radius remains approximately constant in time until the rotational instability causes plasma wall contact and field disruption at $t \sim 50$ μs.

The radial electron temperature profile, determined from Thomson scattering as a function of time on the midplane, is approximately flat at ~ 100 eV for radii less than the separatrix radius until the onset of the rotational instability at $t \sim 30$ μs. Outside the separatrix, $r \sim 6$ cm, the temperature decreases with time from $T_e \sim 70$ eV at 4.5 μs to ~ 10 eV at 30 μs. Doppler broadening measurements of CV give ion temperatures of 200 eV at $t = 10$ μs that approach the electron temperatures in the classical equilibration time of the two species ($t \sim 40$ μs).

The axial density profile was determined from a 6328A laser interferometer that measured the integrated-line density across a diameter as a function of axial position and time. The axial length of the plasma is observed to be about 50 cm in the 1-m length coil and to be relatively constant during the plasma stable period. Excluded flux radius measurements, obtained from a series of loops and probes along the axial direction, indicate the FRC configuration is relatively stationary during the quiescent period and until the rotational instability has grown to cause plasma-wall contact ($t \lesssim 50$ μs).

In the new FRX-C experiment[26] with a deuterium fill pressure of 20 mtorr, the FRC equilibrium is characterized at 20 μs by the following parameters: separatrix radius $r_s \sim 12$ cm, separatrix length $\ell_s \sim 115$ cm, B (external) ~ 7.4 kG, peak density $\sim 4\times10^{15}$ cm^{-3}, $T_e \sim 80$ eV, $T_i \sim 200$ eV, τ_s (stable) ~ 80 μs, and $R/\rho_{i0} = 30$. At a filling pressure of 5 mtorr the equilibrium parameters are: $r_s \sim 9.2$ cm, $\ell_s \sim 100$ cm, B (external) ~ 7.7 kG, peak density $\sim 2.3\times10^{15}$ cm^{-3}, $T_e \sim 100$ eV, $T_i \sim 550$ eV, τ_s (stable) ~ 43 μs, and $R/\rho_{i0} \sim 15$. The lower fill pressure results in well-centered FRCs, but as the fill pressure increases the FRC length becomes comparable to the coil length and often one end or the other of the FRC appears to expand out of the coil.

Theoretical study of FRCs has been impeded by difficulty in computing highly elongated or prolate equilibria of the type observed in field-reversed theta-pinch experiments. Single fluid, scaler pressure models of FRC equilibrium have been developed by a number of workers. Recently Spencer and Hewett[28] have developed a new approach to the computation of FRC equilibria that avoids the previously encountered difficulties. They have computed highly elongated FRC equilibria in a straight conducting cylinder for pressure profile $p'(\psi) = cH(\psi)$, where $H(x)$ is the Heaviside function. The equilibria are found by inverting the Grad-Shafranov equation by means of a Green's function and by solving the resulting non-linear integral equation. Long prolate equilibria are obtained only for values of the constant c very near a critical-value; the equilibria change from 2:1 elongated to infinitely long as c varies by only 0.3%. This critical value of c is predicted by the average beta condition. The elongation and the shape of the separatrix near the field nulls is restricted by the requirement that the field lines outside the separatrix satisfy conducting wall boundary conditions. To change the shape of the transition region it is necessary to either change the boundary conditions or the pressure profile. The sharp singularity in the elongation as a function of the parameter c is not unique to the particular $p(\psi)$ studied and makes looking for long equilibria

by varying parameters in the pressure profiles very difficult.

C. Stability

For highly elongated FRC equilibria having proper profiles and boundary conditions, theory predicts all ideal MHD modes to be stable except for two types: (1) the m=1, n=1 tilt mode;[29] and (2) high n-number axial and radial kinks with poloidal mode number m=1.[25] All FRC experiments with high elongation ($\ell_s/r_s \gg 1$) have exhibited gross stability. No large scale MHD instabilities except rotationally driven ones are observed in the experiments even though the FRC exists for many Alfvén transit times. The tilt mode is not observed except when an FRC is highly contracted axially ($\ell_s/r_s < 3$). Recent theoretical results by Spencer et al.,[30] show that making FRCs racetrack like rather than elliptical stabilizes the tilt mode. The m=1 low n-number radial kink modes are stable provided the FRC separatrix is sufficiently close to the wall. The m=1 high n-number kink modes are not observed in the experiments, and are assumed to be finite Larmor radius (FLR) stabilized. A question for FRCs centers on the trade off between confinement and FLR stabilizing effects since confinement improves as $S = R/\rho_i$ increases and the FLR effects decrease. The FRX experiments have operated with S in the range of 6 to 30.

Most of the FRCs eventually go unstable to an n=2 rotational flute instability where n is the toroidal mode number. The experimental observations are in agreement with predictions of a Vlasov fluid code analysis of this mode;[31] which indicates instability when the plasma rotation exceeds a critical angular velocity. End-shorting and diffusion mechanisms have been proposed as causes of rotational acceleration in the FRCs.[17] End shorting of open field lines on insulating walls by wall plasma provides a path for shorting E_r in the bulk of the plasma. Steinhauer[32] has studied end shorting in FRCs, and finds that the torque applied to the open field-line plasma by end-shorting currents is transmitted across the separatrix to the closed field-line plasma through viscosity.

The diffusion mechanism involves the transfer of net angular momentum through particle loss across the separatrix and then out of the system. Barnes and Seyler[20] have developed a kinematic theory that indicates particles with orbits near the separatrix have a preferred angular momentum. Loss of these particles leaves the closed field-line plasma with a net angular momentum of the appropriate sign. The instability threshold is predicted to occur in the FRX-B plasma when the fraction of particles lost F = 0.57 compared with the experimental observation F = 0.55 ± 16.[18] If the diffusion mechanism is correct, i.e., the radial flow velocity driven by particle transport gives rise to a finite pressure anisotropy in the azimuthal direction resulting in a net torque on the confined plasma, the n=2 rotational mode would not be a limitation for a reactor. Rather, loss of plasma would limit the fusion output before the mode went unstable.

D. Confinement

In the present FRX experiments the onset of the n=2 rotational instability appears to occur on the same timescale as particle diffusion across the separatrix. In the FRX-B experiment the energy confinement time is found to be comparable to the particle confinement time.[36] Therefore, particle loss is thought to be a crucial issue for FRCs. Particle loss has been investigated by Tuszewski and Linford[33] using a steady-state, one-dimensional model for radial particle transport which approximates the experimental obser ation of elongated

FRC equilibrium with approximately constant separatrix radius. It is found that anomalous transport from the lower-hybrid-drift (LHD) instability[34] with the wave energy bound on the saturation level dominates the particle confinement over classical effects, particularly for larger devices. This analytical result is in qualitative agreement with a one-dimensional anomalous transport code developed by Hamasaki.[35] The code incorporates in its transport coefficients, contributions from classical processes as well as from the LHD instability, the latter contribution being dominant.

E. Scaling

Scaling studies of plasma behavior and parameters have been performed in the FRX-A and -B experiments,[36,37,17] and are underway in the larger FRX-C[26] device. The variation of the FRC stable configuration time, τ_s, with plasma parameters is of particular interest. Data from the FRX experiments show that τ_s scales as $\tau_s \simeq 6.0\times10^{-7}\ R^2/\rho_i$. The experiments also indicate that τ_s is insensitive to the ion temperature when R^2/ρ_i is held approximately constant. The one-dimensional, Lagrangian, transport model of Hamasaki,[35] with the quasi-linear diffusion coefficient for the LHD instability, has indicated that the time for half the particle inventory to be lost across the separatrix scales as R^2/ρ_{io}, but is independent of the ion temperature. The particle and energy confinement times determined from the FRX-B experiments[17] are in approximate agreement with the Hamasaki code results. The linear scaling of τ_N with the plasma density scale parameter R^2/ρ_i indicated by the code and the experimental correlation of τ_s with these parameters suggest that $\tau_s \propto \tau_N$. This agreement supports the hypothesis of the rotational acceleration being driven by diffusion.

REFERENCES

1. W. T. Armstrong, et al., Proc. 8th Internl. Conf. on Plasma Phys. and Contr. Nucl. Fusion Res., (IAEA, Vienna, 1980) Vol. I, 481.
2. T. R. Jarbo, et al., Phys. Rev. Lett. 45, 1264 (1980).
3. H. Alfvén, et al., J. Nucl. Energy, Part C 1, 116 (1960).
4. M. N. Rosenbluth and M. N. Bussac, Nucl. Fusion 19, 489 (1979).
5. J. B. Taylor, Phys. Rev. Lett. 33, 1139 (1974), and Proc. 3rd Topical Conf. High Beta Plasmas, (Pergamon, Oxford, 1976) p. 59.
6. D. A. Baker and W. E. Quinn, Fusion (ed. E. Teller), Vol. I, Ch. VII, p. 445. Academic Press, New York, 1981.
7. A. G. Sgro, private communication.
8. H. W. Hoida, et al., Proc. IEEE Internl. Conf. on Plasma Science Ottawa, 1982).
9. C. W. Barnes, et al., Proc. IEEE Internl. Conf. on Plasma Science (Ottawa, 1982).
10. J. M. Finn and A. Reiman, Proc. 3rd Symposium on Phys. and Tech. of Compact Toroids (Los Alamos, 1980) p. 64 (1981).
11. S. C. Jardin, Proc. U.S.-Japan Workshop on Compact Toroids (Osaka, 1981) p. 125 (1981).
12. W. C. Turner, et al., Proc. 3rd Symposium on Phys. and Tech. of Compact Toroids (Los Alamos, 1980) p. 113 (1981).
13. H. H. Fleischmann, Proc. U.S.-Japan Symposium on Compact Toruses and Energetic Particle Injection (Princeton, 1979) p. 41 (1980).
14. M. Okabayashi and A. M. M. Todd, Nucl. Fusion 20, 571 (1980).
15. G. C. Goldenbaum et al., Phys. Rev. Lett. 44, 393 (1980).
16. I. Henins et al., Proc. 3rd Symposium on Phys. and Tech. of Compact Toroids (Los Alamos, 1980) p.101 (1981).

17. W. T. Armstrong et al., Phys. Fluids 24, 2068 (1981).
18. R. K. Linford et al., Plasma Phys. and Controlled Nucl. Fusion Res. (IAEA, Vienna, 1978) Vol. II, p. 447.
19. A. G. Es'kov et al., Plasma Phys. and Controlled Nucl. Fusion Res. (IAEA, Vienna, 1978) Vol. II, p. 187.
20. D. C. Barnes and C. E. Seyler, Proc. U.S.-Japan Symposium on Compact Toruses and Energetic Particle Injection (Princeton, 1979) p. 110.
21. V. N. Semenov and N. V. Sosnin, Sov. J. Plasma Phys. 7, 180 (1981).
22. D. C. Barnes and C. E. Seyler, Los Alamos Scientific Laboratory report LA-UR-79-13 (1979).
23. A. I. Shestakov et al., Proc. U.S.-Japan Symposium Compact Toruses and Energetic Particle Injection (Princeton, 1979) p. 126.
24. D. V. Anderson and D. C. Barnes, Phys. Rev. Lett. 46, 1337 (1981).
25. W. Newcomb, Phys. Fluids 23, 2296 (1980).
26. R. R. Bartsch et al., Proc. IEEE Internl. Conf. on Plasma Science (Ottawa, 1982).
27. A. L. Hoffman, Mathematical Sciences Northwest report 80-1144-4 (1982).
28. R. L. Spencer and D. W. Hewett, to be published, Phys. Fluids. Also Los Alamos National Laboratory report LA-UR-82-330 (1982).
29. D. C. Barnes et al., Proc. 3rd Symposium on Phys. and Tech. of Compact Toroids (Los Alamos, 1980) p. 134 (1981).
30. R. L. Spencer et al., Proc. Sherwood Theory Meeting (Santa Fe, 1982) paper 8.3.
31. C. E. Seyler, Phys. Fluids 22, 2324 (1979).
32. L. C. Steinhauer, Proc. U.S.-Japan Symposium on Compact Toruses and Energetic Particle Injection (Princeton, 1979) p. 151.
33. M. Tuszewski and R. K. Linford, to be published Phys. Fluids.
34. R. C. Davidson and N. A. Krall, Nucl. Fusion 17, 1313 (1977).
35. S. Hamasaki and N. A. Krall, Proc. IEEE Internl. Conf. on Plasma Science (Montreal, 1979) paper 5E10.
36. J. Lipson et al., Appl. Phys. Lett. 39, 43 (1981).
37. W. T. Armstrong et al., Proc. 4th U.S.-Japan Workshop on Compact Toroids (Livermore, 1981).

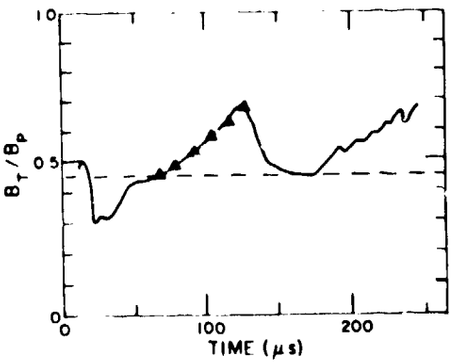

Fig. 1. Plot of the ratio of the measured (solid line) toroidal field to poloidal field as a function of time in the CTX spheromak. The triangular points are computed using a 2-D transport code.